CrossMark

Removal of uranium(VI) and thorium(IV) by insolubilized humic acid originated from Azraq soil in Jordan

Fawwaz I. Khalili[1] · Alia'a Khalifa[1] · Ghadeer Al-Banna[1]

Abstract Humic acid from Azraq soil in Jordan has been extracted and insolubilized as the sodium form (INaAZHA). It was characterized by Fourier transform infrared spectroscopy, elemental analysis, thermal gravimetric analysis, X- ray diffraction, scanning electron microscopy and differential scanning calorimetry. Sorption of Th(IV) and U(VI) by INaAZHA was studied using batch and column. The kinetic studies fitted pseudo second–order kinetic model. The data were fitted to Langmuir, Freundlich and Dubinin–Radushkevich (D–R) sorption isotherms. Thermodynamic functions, $\Delta G°$, $\Delta H°$ and $\Delta S°$ were determined for the sorption. Desorption from column was best using 1.0 M than 0.5 and 0.1 M HNO$_3$ for both.

Keywords Azraq humic · Insolubilized · Sorption · Kinetic · Thermodynamic · Thorium(IV) · Uranium(VI)

Introduction

The occurrence of uranium and thorium in soil, rocks, groundwater, is a serious problem from the environmental viewpoint. Uranium and thorium presence in the environment can be hazardous to health. Cellular and animal studies have shown that uranium is a kidney toxin, neurotoxin, immunotoxin, mutagen, carcinogen, and teratogen [1]. Where, the main radiological hazard from uranium is alpha radiation. When it is inhaled or ingested, alpha radiation is the most damaging form of ionizing radiation

[1]. The solid and liquid effluents containing Th(IV) are known to cause acute toxicological effects and harmful diseases for human such as lung, pancreatic and liver cancer through inhalation, smoking and oral intake [2]. Uranium and thorium are very essential elements in nuclear energy programs. Their separation and recovery are essential to minimize their discharge into the environment from the point of view of safety and economy [3]. In Jordan, there are several sites contain considerable reserves of uranium and thorium ores [4]. Enhanced levels of uranium and thorium and their daughter products might be present in ground water in areas that are rich in natural radioactivity. The earth's crust in Jordan is covered by phosphate rocks that could make the water sources rich in ^{238}U and its daughters which may be found dissolved or suspended in the water [5]. Various techniques are employed for the removal and separation of radionuclides (uranium and thorium), such as precipitation, ion exchange, solvent extraction, and sorption [2]. Sorption is the process that involves nothing more than the preferential partitioning of substances from the gaseous or liquid phase onto the surface of solid substrate; the sorption phenomenon has become a useful tool for purification and separation [2].

The sorption procedures mainly involve the development of low cost adsorbents over a wider range of pH values at lower concentrations with easy manipulation and regeneration for possible reuse [6–8]. Many researchers have used various solids, which are natural, organic, and inorganic; for example, coir pith, zeolite, activated carbon, cement, alumina, silica, and natural substances like organic matter (humus) and clay minerals [4, 7–10].

Humic substances (HS) are a series of naturally occurring high molecular weight compounds, which are the main component of organic matter in soils and waters. The humic substances can be classified according to their

✉ Fawwaz I. Khalili
fkhalili@ju.edu.jo

[1] Chemistry Department, The University of Jordan, Amman 11942, Jordan

solubility characteristics in aqueous media, and generally three main subclasses are considered: humic acids (HAs), the soluble fraction of HS at high pH values; fulvic acids (FAs), the soluble fraction of HS under all pH conditions and humin, the insoluble fraction of HS at any pH value [11]. (HSs) represent about 50–80 % of natural organic matter (NOM) in water, soil and sediment [12].

In term of capacity and rate of sorption, HA is a very good sorbent for various metal cations. This is why that in context of environmental preservation, the high ability of HA in binding metal cations is a primary concern [13].

The Azraq humic acid (AZHA) was found to be the most developed HA (high %C and high molecular mass) in comparison with HAs from other locations in Jordan [14]. X-ray studies of AZHA showed that it has a non-crystalline amorphous and irregular heteropolycondensates [15]. Solution ^{13}C-NMR studies indicated that AZHA has significant aliphatic moieties [16]. AZHA has been extracted by various extractants, such as 0.5 M NaOH, 0.1 M NaOH, 0.1 M $Na_4P_2O_7$ (at 25 and 50 °C), 0.1 M NaOH + 0.1 M $Na_4P_2O_7$ and 0.1 M NaF (at 25 and 50 °C) solutions. The obtained HA samples were characterized by elemental analysis, UV–Vis, FTIR, X-ray Diffraction, Differential Thermogravimetry, and solution and solid ^{13}C-NMR. The diversity in characteristics of HAs obtained indicates either that the extractants alter HA during extraction or that there are several forms of HA in soil [17].

Mohammad and Khalili [18] studied the sorption of thorium(IV) and uranium(VI) onto Azraq humic acid (AZHA), they found that as pH increases the adsorptivity of metal ions increases. The order of adsorptivity of thorium(IV) and uranium(VI) onto AZHA was found to be thorium(IV) is greater than uranium(VI)

Al-Banna and Khalili [10] studied the sorption of uranium(VI) and thorium(IV) by insolubilized humic acid (IHA) that extracted from Ajloun soil at different temperatures, and at different pH values, it was found that IHA has higher uptake for Th(IV) than U(VI), and also found the metal ion uptake by IHA increased with pH. The kinetic studies showed that the equilibrium time for each metal ion occurs at 6 h to achieve maximum uptake level. Sorption data were evaluated according to the pseudo second-order reaction kinetic. Thermodynamic data showed that the sorption process is not highly favorable where the value of $\Delta G°$ was positive, while $\Delta H°$ values indicated that this process is endothermic. On the other hand, the process has positive entropy which means that the sorption process increases the disorder of the system and it is entropy driven.

Celebi et al. [19] studied the sorption of radioactive cesium and barium ions onto sodium form of insolubilized humic acid as a function of time, cation concentration, and temperature. The sorption processes are well described by both Freundlich and Dubinin–Radushkevich type isotherms. Thermodynamic constants were determined. It was found that Ba(II) was adsorbed five times more than Cs(I) onto structurally modified humic acid and kinetic studies indicated that sorption behavior of both ions obey the pseudo second order rate law. Structural changes were determined using Fourier transform infrared spectroscopy (FTIR) and Carbon-13 nuclear magnetic resonance (^{13}C NMR) techniques during modification of humic acid. The amount of sorption sites (carboxylic and phenolic groups) decreased during insolubilization process.

The sorption of Th(IV) to bentonite as a function of pH, ionic strength, and humic substances (HSs) was studied by using batch experiments. They found that, the sorption of Th(IV) on Na-bentonite depended greatly on pH and ionic strength, ion exchange and outer-sphere complexes dominated at low pH; whereas inner-sphere complexes and surface precipitation were taking an important role in Th(IV) sorption process; foreign cations with different radii and charges influenced the sorption of Th(IV) on Na-bentonite significantly. The presence of humic substances (HSs) could enhance Th(IV) sorption at low pH but inhibited at high pH mainly because of competition between surface complex and soluble binary complexes. High temperature is advantageous for Th(IV) sorption to Na-bentonite, Langmuir model fits the sorption data better than Freundlich model [20].

The sorption characteristics of copper ions onto insolubilized humic acid by using a continuously monitored solid phase extraction (SPE) technique were studied; where the sodium form of the insolubilized humic acid was found to be effective for (SPE) of metal ions in aqueous media as a reusable solid phase, being insoluble within the pH range of 1–10. The pH and concentration of the loading solution influenced the amount of the Cu(II) sorbed which increased with increasing of pH and concentration of the loading solution. The sorption of Cu(II) in/on Neha was found to be mainly based on ion-exchange and physical interactions, and this was confirmed by the results of sorption isotherms and Scatchard plot analysis. From the Dubinin–Radushkevich (D–R) isotherm, the mean free energy of sorption was calculated as 9.28 kJ mol^{-1}, and this value was attributed to a sorption mainly resulting from ion-exchange and simple dispersive interactions. HA can be used as not only an inexpensive but also as an effective solid/stationary phase for separation, pre-concentration and removal of metal ions in aqueous media [21].

Al-shaybe and Khalili [22] studied the sorption of Th(IV) and U(VI) onto the Jordanian zeolite, the result showed that there are high initial rate of metal ions uptake was observed after 24 h of shaking, and the uptake have increased with increasing pH. Sorption data was evaluated according to the pseudo second-order reaction kinetic,

while sorption isotherms were studied at temperature 25, 35 and 45 °C. The Langmuir, Freundlich and (D–R) sorption models were applied, and the proper constants were derived. It was found that the adsorptivity process is enthalpy driven for thorium(IV) and uranium(VI). Recovery of thorium(IV) and uranium(VI) ions after sorption was carried out by treatment of the loaded zeolitic tuff in the column with 0.1 M HNO_3, 0.2 M H_2SO_4, 0.5–5 × 10^{-5} M EDTA, and 0.1 M sodium acetate. The best percent recovery for thorium(IV) was obtained when 5 × 10^{-5} M EDTA was used, while for uranium(VI) when 0.2 M H_2SO_4 was used.

The sorption behavior of Jordanian bentonite towards U(VI) and Th(IV) in aqueous solutions was studied by batch experiment as a function of pH, contact time, and temperature and by column technique at 25.0 °C and pH 3. The highest rate of metal ions uptake was observed after 18 h of shaking, and the uptake have increased with increasing pH. Bentonite has shown good metal ion uptake capacity toward these metal ions. It was found that the sorption process is enthalpy driven for U(VI) and Th(IV) [4].

The aim of this study is to prepare insolubilized HA from Azraq soil and then to use it as an adsorbent for U(VI) and Th(IV) ions from aqueous solutions. The INaAZHA will be characterized by Fourier transform infrared (FTIR) spectroscopy, thermal gravimetric analysis (TGA), differential scanning calorimetry (DSC), and elemental analysis. Sorption of U(VI) and Th(IV) onto INaAZHA will be studied using batch technique at different pH values (1.0, 2.0, and 3.0), different temperatures (25.0, 35.0 and 45.0 °C), contact time, and at constant ionic strength. To understand and explain the nature of sorption process the data will be analyzed based on sorption models such as: Langmuir, Freundlich, and Dubinin–Radushkevich sorption isotherms. The kinetic and thermodynamic parameters of sorption will be calculated. The desorption process after sorption will be also be studied using column technique.

Theory

Sorption isotherm

Sorption is often described in terms of isotherm models, which show the relationship between the bulk aqueous phase concentration of adsorbate and the amount adsorbed at constant temperature. Isotherms reflect equilibria. Several models have been published to describe experimental data on sorption isotherms. The Langmuir, Freundlich and D–R models are commonly used for describing sorption equilibrium for water and waste- water treatment applications [23].

Langmuir model

The Langmuir sorption model is based on the assumption that all the sorption sites are energetically identical and sorption occurs on a structurally homogeneous adsorbent [24].

The Langmuir equation is expressed as:

$$q_e = q_m K_L C_e / (1 + K_L C_e) \qquad (1)$$

The linear forms of the Langmuir equation are written as follows:

$$C_e / q_e = 1/(q_m K_L) + (1/q_m) C_e \qquad (2)$$

where q_e is the amount of solute adsorbed per unit weight of adsorbent (mg g^{-1}), C_e is the equilibrium concentration of solute (mg L^{-1}), q_m is the sorption capacity (mg g^{-1}), or monolayer capacity, and K_L is the Langmuir equilibrium constant related to the affinity of binding sites and energy of sorption (L mg^{-1}) [25]. The values of q_m and K_L can be evaluated from the slope and the intercept of the linear plot of experimental data of C_e/q_e versus C_e, Eq. (2).

Freundlich model

Freundlich expression is an empirical equation applicable to non-ideal sorption on heterogeneous surface as well as multilayer sorption. The model is given as

$$q_e = K_F C_e^{1/n} \qquad (3)$$

K_F is a constant indicates relative sorption capacity, while $1/n$, is indicative of the energy or intensity of the reaction and suggests the favorability and capacity of the adsorbent/adsorbate system. Where, $n > 1$ represents favorable sorption conditions. Equation (4) is linearized into logarithmic form for data fitting and parameter evaluation, as follows:

$$\log q_e = \log K_F + 1/n \log C_e \qquad (4)$$

By plotting $\log q_e$ versus $\log C_e$, constant K_F and exponent $1/n$ can be calculated from the intercept and slope respectively [18, 26].

Theoretically, the Freundlich equation represents a situation in which the quantity of solute adsorbed increases indefinitely with increasing concentration [27].

Dubinin–Radushkevich (D–R) model

D–R isotherm is commonly used to describe the sorption isotherm of single solute system, although this is analogue to Langmuir model, D–R model is more general than Langmuir as it rejects the homogenous surface or constant sorption potential [28]. D–R sorption isotherm is applied to

distinguish between chemical and physical sorption and it is valid at low concentration ranges [29].

$$\ln q = \ln q_{max} - \beta \varepsilon^2 \tag{5}$$

β is the activity coefficient related to mean sorption energy (mol² kJ⁻²), ε is the Polanyi potential.

$$\varepsilon = RT \ln(1 + 1/C_e) \tag{6}$$

where R is the ideal gas constant (8.3145 J mol⁻¹ K⁻¹) and T is the absolute temperature in Kelvin [30]. The sorption free energy (E), Eq. (7), is defined as the free energy change required for transferring one mole of ions from solution to solid surface, this energy is calculated as follows:

$$E = 1/(2\beta)^{0.5} \tag{7}$$

The magnitude of E can give a good idea about the mechanism of the sorption. If E is in the range of 8–16 kJ mol⁻¹, the sorption is governed by chemical ion exchange, but in the case of $E < 8$ kJ mol⁻¹, physical forces may affect the sorption. On the other hand, sorption may be dominant by particle diffusion if $E > 16$ kJ mol⁻¹ [29].

Sorption kinetics

The amount of metal adsorbed by INaAZHA was calculated using the following equation:

$$q_e = (C_i - C_e) \times V/m \tag{8}$$

where q_e is the metal uptake (mg g⁻¹), C_i and C_e are the initial and equilibrium metal concentrations in the solution (mg L⁻¹), respectively, V is the solution volume (L), and m is the mass of adsorbent (g).

The distribution coefficient (K_d) (L g⁻¹) of metal ions between the aqueous phase and the solid phase can be directly obtained using:

$$K_d = q_e/C_e \tag{9}$$

The K_d value was obtained from the intercept of the plot of $\ln(q_e/C_e)$ versus q_e [30].

In order to understand the sorption process of U(VI) and Th(IV) metal ions onto the adsorbent (INaAZHA), two kinetic models, pseudo-first- and second-order models, were proposed.

Pseudo-first-order reaction kinetic

The pseudo-first-order equation can be written as:

$$dq_t/dt = k_1(q_e - q_t) \tag{10}$$

where q_t (mg g⁻¹) is the amount of adsorbate absorbed at time t (min), q_e (mg g⁻¹) is the sorption capacity in equilibrium, and k_1(min⁻¹) is the rate constant for pseudo-first-order model. After integration and by applying the initial conditions $q_t = 0$ at $t = 0$ and $q_t = q_e$ at $t = t_e$, the equation becomes:

$$\ln(q_e - q_t) = \ln q_e - k_1 t \tag{11}$$

Thus, a plot of $\ln(q_e - q_t)$ against t should be a straight line with slope $= -k_1$ and an intercept $= \ln q_e$ [31].

Pseudo-second order reaction kinetic

The pseudo-second-order model can be presented in the following form:

$$t/q_t = 1/k_2 q_e^2 + t/q_e \tag{12}$$

where k_2 is the rate constant of pseudo-second-order model in unit of g mg⁻¹ min⁻¹.

Thus, a plot of t/q_t against t should be a straight line with slope $= 1/q_e$ and an intercept $= 1/(k_2 q_e^2)$ [28]. The validity of pseudo-first-order or pseudo-second-order kinetics can be tested by comparing values of the experimental q_e values with the calculated values [31, 32].

Activation parameters for sorption

The activation energy (E_a; kJ mol⁻¹) is required to bring the reactants to a condition necessary to form the products, according to Arrhenius's equation:

$$\ln k = -E_a/RT + \ln A \tag{13}$$

where $k = k_2$ (min⁻¹) is the pseudo-second-order rate constant at the (absolute) temperature T, the constant A is called a frequency factor and contains information about molecular collision frequency [33]. A plot of $\ln(k)$ versus $1/T$ gives a straight line whose slope is equal to $(-E_a/R)$ and the intercept on the ordinate gives $\ln(A)$.

The magnitude of the activation energy gives an idea about the type of sorption. Low activation energies (5–50 kJ mol⁻¹) are characteristics for physical sorption, while higher activation energies (60–800 kJ mol⁻¹) suggest chemical sorption [34].

To calculate the thermodynamic activation parameters such as enthalpy of activation, $\Delta H^{\ddagger}$, entropy of activation $\Delta S^{\ddagger}$, and free energy of activation $\Delta G^{\ddagger}$, the Eyring Eq. (14) was applied.

$$\ln(k_2/T) = \left[\ln(k_B/h) + \Delta S^{\ddagger}/R\right] - \Delta H^{\ddagger}\Big/R(1/T) \tag{14}$$

where k_B is the Boltzmann constant (1.3807 × 10⁻²³ J K⁻¹), h is the Planck constant (6.6261 × 10⁻³⁴ J s), k_2 is the pseudo-second-order constant for metal ions sorption [35]. The plot of $\ln(k_2/T)$ versus $1/T$ gives a straight line with slope $-\Delta H^{\ddagger}/R$ from

which the enthalpy of activation can be derived and with intercept $\ln (k_B/h) + \Delta S^{\ddagger}/R$ from which the entropy of activation is calculated [36].

The calculated value of the entropy of activation is used for the suggestion of a mechanism i.e. in replacement reactions, associative ($\Delta S^{\ddagger} < 0$), dissociative ($\Delta S^{\ddagger} > 0$), and interchange ($\Delta S^{\ddagger} = 0$) [36]. The positive value of $\Delta H^{\ddagger}$ confirms the endothermic process, meaning the reaction consume energy, while the negative value of $\Delta H^{\ddagger}$ confirms the exothermic process [34].

Calculation of $\Delta G^{\ddagger}$ for the appropriate reaction temperature is allowed according to Eq. (15).

$$\Delta G^{\ddagger} = \Delta H^{\ddagger} - T\Delta S^{\ddagger} \tag{15}$$

The positive $\Delta G^{\ddagger}$ value suggests that the sorption reactions require energy to convert reactants into products and vice versa. The $\Delta G^{\ddagger}$ value determines the rate of the reaction, rate increases as $\Delta G^{\ddagger}$ decreases.

Experimental

Materials

All reagents used in this study were of analytical grade reagents. Sodium hydroxide (NaOH) from LOBA, hydrochloric acid 37 % (HCl) and nitric acid 69 % (HNO₃) from TEDIA, sodium perchlorate (NaClO₄) from Acros, thorium nitrate tetrahydrate (Th(NO₃)₄·4H₂O) from Riedel-De-Haen, uranyl nitrate hexahydrate (UO₂(NO₃)₂·6H₂O) from BDH Chemicals Ltd and Arsenazo(III) indicator from Fluka. Azraq Oasis is located in the eastern desert of Jordan 100 km east of Amman and has a total area of about 26 km², where there is a plenty of plants, water, animal and bird life, and warm weather. These are the best conditions for the formation and the development of Humic Acid (HA) [16]. The soil sample used in this study was collected from the A0 (top layer) horizon which lies cross the street from Qasr Al-Azraq next to the water pump (North Azraq). The soil has a dark black color.

Instrumentation

Weighing of samples was done by using AW120 Electronic Balance. The pH of the solutions was measured with a METROHM 605 pH-meter. FTIR spectrum of INaAZHA was recorded using Thermo Nicolet NEXUS 670 FT-IR Spectrophotometer. Elemental analyses of the INaAZHA sample was done by using Euro Vector 3000 Elemental Analyzer. The thermal gravimetric analysis (TGA) of the INaAZHA sample was studied using NETZCH STA 409 PG/PC Thermal Analyzer in the temperature range

(25–800 °C), at a heating rate of 20 °C min⁻¹. XRD of INaAZHA samples were recorded using Philips X pert PW 3060, operated at 45 kV and 40 mA. The shape and surface morphology of the INaAZHA was examined with The FEI inspect F50 scanning electron microscope, the energy dispersion spectrum (EDS) was used to determine the elements present. Shaking of samples was done using Clifton shaker equipped with thermostat. The concentrations of the metal ions were determined using UV–VIS Spectrophotometer from Spectroscan model 80DV.

Extraction of humic acid from Azraq soil

Humic acid used in this work (after insolubilization) were extracted from a soil sample collected from the A0 (top layer) horizon which lies cross the street from Qasr Al-Azraq next to the water pump lake (North Azraq–Jordan). The soil samples were air dried, crushed and homogenized prior to extraction. Humic acid was extracted from Azraq soil sample by the following procedure: 300 g of soil was extracted with 3.0 L of 0.5 M NaOH for 24 h at room temperature. The mixture was filtered through Whatman filter paper (100) after that the supernatant was acidified with HCl to pH 1.0 and left at room temperature for 24 h. The resulting precipitate was rinsed many times with deionized water to remove chloride ions. The precipitate was dried at 95 °C in the oven for 4 h. Then it was insolubilized by heating it at 330 °C for 1.5 h, then the solid (IAZHA) was homogenized by converting it to its sodium form (INaAZHA) by stirring in a 1 M NaNO₃ solution for 48 h. The resulting solid phase (4.44 g) was dried at 80 °C [19]. The percentage yield for INaAZHA from soil according to this procedure is 1.48 % (14.81 g INaAZHA kg⁻¹ soil⁻¹). The total number of grams that obtained from 3.50 kg Azraq soil sample was 51.84 g.

Characterization of insolubilized Azraq humic Acid

The INaAZHA was characterized by Fourier transform infrared (FTIR) spectroscopy, differential scanning calorimetry (DSC), thermal gravimetric analysis (TGA), elemental analysis, X-ray diffraction (XRD), and the shape and surface morphology was studied by scanning electron microscopy (SEM).

Preparation of stock solutions

Stock solutions of 2000 ppm for the two metal ions were prepared separately by dissolving specific amount of each metal salt of Th(IV) and U(VI) in 0.1 M NaClO₄ (to keep ionic strength constant). The stock solutions were used to prepare solutions with different concentrations (10, 20, 25, 30, 35, and 40 ppm), the dilution is achieved by using

0.1 M $NaClO_4$ and 0.1 M $HClO_4$ solutions at different pH 1.0, 2.0 and 3.0.

Spectrophotometric procedure for Th(IV) and U(VI)

Preparation of Arsenazo (III) indicator solution

A 0.10 % aqueous solution of Arsenazo(III) was used as a spectrophotometric reagent in the determination of thorium(IV) and uranium(VI) concentration.

Spectrophotometric determination of Th(IV) and U(VI) ions

A 0.5 mL of the aqueous test solution of Th(IV) were added in 25 mL volumetric flask, then 10 mL of 9.0 M Hydrochloric acid solution were added, then 0.5 mL of Arsenazo(III) indicator was transferred and dilution was done to the mark with deionized water [37]. The spectrophotometric determination was carried out within 1 h of sample preparation at 660 nm wavelength for Th(IV). A 4.0 mL of the aqueous test solution of U(VI) were added in 50 mL volumetric flask, then 20 mL of 0.01 M Hydrochloric acid solution were added, then 1 mL of Arsenazo(III) indicator was transferred and dilution was done to the mark with deionized water [38]. The spectrophotometric determination was carried out within 1 h of sample preparation at 650 nm wavelength for U(VI).

Sorption experiments

Kinetic studies

A calibration curve was determined using a series of standard solutions prepared from metal nitrates in 0.10 M $NaClO_4$ prior to measurements.

Experiments for determination of the equilibrium time of the sorption process was studied by shaking 50.0 mg ± 0.1 mg of the INaAZHA with 50.0 mL (transferred to Pyrex glass flasks) of 30 mg L^{-1} metal ion solution at pH 3.0, the contact time was varied from 15 min to 72 h at (25.0, 35.0 and 45.0 °C). The mixture was filtered and the concentration of the metal ion remaining was determined spectrophotometrically. From these experiments we can also found the activation energy, via knowledge of the rate constants of interaction of metal ions with INaAZHA at different temperatures.

Sorption isotherms

The sorption of Th(IV), and U(VI) was carried out by taking a known mass of 50.0 mg ± 0.1 mg of the

INaAZHA with 50.0 mL of solutions of concentration variation ranging as (10, 20, 25, 30, 35, 40) mg L^{-1} for each metal, under different pH values of 1.00, 2.00 and 3.00; and at different temperatures (25.0, 35.0 and 45.0 °C). All samples were shaken using shaker for 24 h.

Metal ion-uptake by the INaAZHA using column experiment

Glass column of 20 cm length, and 20 mm inner diameter was used in this experiment. The column was packed with 2000.0 ± 0.1 mg dried INaAZHA. A sample volume of 50.0 mL containing Th(IV) of 1000 mg L^{-1} was passed through the column at a flow rate of 0.5 mL min^{-1}. The eluate was collected in a 100.0 mL conical flask, and concentration of the metal ion was then determined by UV–Vis. The same experimental conditions were used for the determination of U(VI) ions uptake. Every measurement was repeated three times to make sure of the accuracy and reproducibility of the results, then average was taken.

Desorption studies

The desorption of the Th(IV), and U(VI) ions was carried under column condition, where the INaAZHA was loaded with each metal ion as described previously, using 50.0 mL of three eluting agents, 1, 0.5 and 0.1 M HNO_3 were used for INaAZHA recovery from adsorbed metal ion, keeping the flow rate of elution at (0.5 mL min^{-1}). The concentration of metal ion in the eluate was collected in five 10.0 mL portions, and was then determined by the UV–Vis spectrophotometer

Results and discussion

Characterization and analysis of insolubilized Azraq humic acid samples

Insolubilized Azraq humic acid (INaAZHA) samples were characterized using X-ray diffraction (XRD), Fourier transform infrared (FTIR) spectroscopy, thermogravimetric analysis (TGA), differential scanning calorimetry (DSC), elemental analysis, and scanning electron microscope (SEM).

XRD characterization

The XRD patterns for the INaAZHA (a) pure (b) with adsorbed thorium and (c) with adsorbed uranium are presented in Fig. 1. From Fig. 1a we can note that the appearance of the band at $2\theta = 19.67°$, is attributed to aliphatic or condensed saturated rings [39, 40]. The band at

Fig. 1 XRD pattern for INaAZHA **a** pure, **b** with adsorbed thorium and **c** with adsorbed uranium
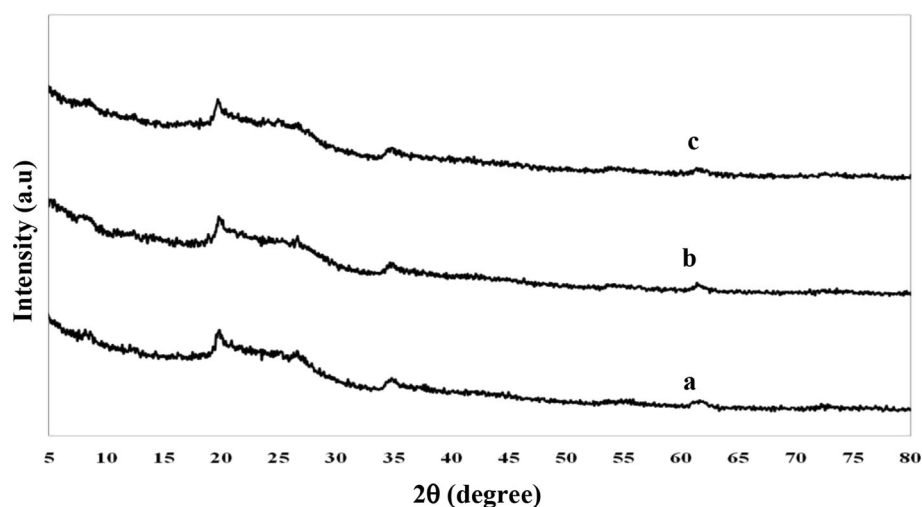
about $2\theta = 24.59°$ of INaAZHA indicate condensed aromatic carbons [40]. The INaAZHA showed band at $2\theta = 27°$, the appearance of this band is a typical feature of a graphite–like structure [39]. The band at $2\theta = 34.98°$ is due to the aromatic structure which indicate the existence of the graphite like layers [39].

$2\theta = 27°$, the appearance of this band is a typical feature of a graphite–like structure. The band at $2\theta = 34.98°$ is due to the aromatic structure which indicate the existence of the graphite like layers [39].

From the same Fig. 1b, c we can see that the structure of INaAZHA is not affected by the presence of adsorbed metal ions Th(IV) and U(VI), this due to the graphite like structure of INaAZHA, also this confirms that sorption of this metals occurs at the surface of INaAZHA.

Fourier transform infrared (FTIR) spectra

Insolubilized Azraq humic acid (INaAZHA) was characterized by FTIR. This technique could be used to identify the major functional groups present in INaAZHA. The peaks in FTIR spectrum shown in Table 1 are as follows; a broad band at 3898 cm^{-1} primarily corresponds to O–H stretching and secondarily to N–H stretching, absorption bands at 2925 and 2837 cm^{-1} are attributed to aliphatic C–H stretching in CH$_2$ and CH$_3$, respectively. The absorption band at 1709 cm^{-1} is due to C=O stretching of carboxylic acid and ketone, the absorption bands at 1605 and 1368 cm^{-1} are ascribed to stretching of carboxylate, these peaks indicate the presence of sodium ion in the INaAZHA structure, as a result to the treatment of INaAZHA with 1 M NaNO$_3$ for 48 h, and the peak at 1605 cm^{-1} can also be attributed to vibrations of aromatic C=C bonds. The peak at 1221 cm^{-1} represents C–O stretching in phenols and O–H deformation of COOH. The deformation of aliphatic C–H and, H–bonded C=O of conjugated ketones and water deformation occurs at 1458 cm^{-1}, the band at 1032 cm^{-1} represents C–O stretching of polysaccharides. This FTIR spectrum agrees with FTIR spectra of IHA from Ajloun [10].

Table 1 FT-IR peaks position (cm^{-1}) for INaAZHA

Position (cm^{-1})	Corresponding response
3402	O–H vibrations and N–H vibrations
2929 and 2850	Stretching of aliphatic C–H groups
1720	C=O stretching of various carbonyl groups including COOH
1631	C=C aromatic and olefinic vibrations, C=O stretching of amide groups, conjugated ketones, and COO$^-$ symmetric stretching
1510	C=C stretching and/or N–H deformation
1463	O–H deformation, C=O stretching of phenolic groups and aliphatic C–H deformation of structures such as fatty acids and waxes
1033	C–O stretching of polysaccharides like compounds and/or to Si–O silicate impurities
914 and 793	Out of plane bending of aromatic C–H

Thermal properties

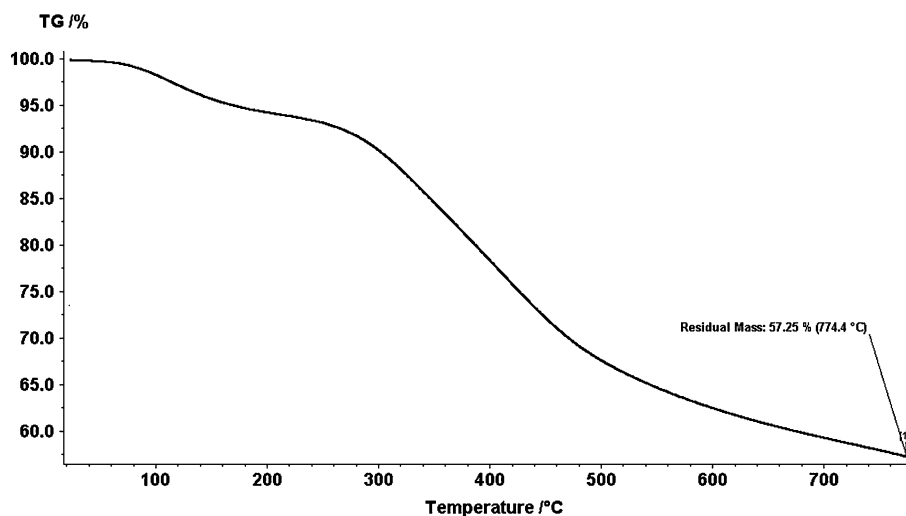### Thermogravimetric analysis (TGA)

The thermal stability of the INaAZHA was investigated by thermogravimetric analysis (TGA) under dry nitrogen atmosphere, and differential scanning calorimetry (DSC). The TGA curve (Fig. 2) displayed two-step weight loss. The first step is below 150.0 °C, which could be due to dehydration [41], this loss of mass is associated also with partial decomposition of aliphatic groups.

The extra weight loss occurring at temperature between 150.0 and 500.0 °C could be attributed to decarboxylation of the humic material, and extensive decomposition of aliphatic structures, deterioration of alcoholic, phenolic, amino groups, and decomposition of aromatic structures [10, 42]. The TGA curve showed the residual mass percentage at 774.4 °C equal to 57.25 % for INaAZHA, which may be due to the presence of sodium in INaAZHA, metal oxides and silicate impurities. Previously, the TGA curve of Ajloun IHA was reported to show the residual mass percentage of 70.23 % at 901.4 °C which was due to metal oxides and silicate impurities [10].

Differential scanning calorimetry (DSC)

Figure 3 shows two major endothermic peaks, the first peak at 96.50 °C is the melting peak which due to the melting of lipid fraction of humic acid, aliphatic components of lipid fraction appear similar to polymethylene chains with semi crystalline character that are analogous to polyethylene [43]. Broad endothermic peak suggest that a more heterogeneous mixture of compounds is present [43]. The peak at 485.2 °C ascribed to the decomposition of aromatic structures of INaAZHA, as shown by IHA from Ajloun area [10].

Elemental analysis

Elemental analysis was done to show the percentage of each element in the INaAZHA. Table 2 shows the percentage of each element in the INaAZHA and AZHA [14].

Percentages (%) of carbon, nitrogen, and hydrogen in INaAZHA is less than AZHA, which may be due to decarboxylation of humic acid and extensive decomposition of aliphatic structures upon heating to 330 °C for 1.5 h [17]. Also, the presence of sodium (INaAZHA) may leads to decrease in the %C. We note the %C is lower for Ajloun IHA in comparison with AZHA and INaAZHA, which may be due to the presence of metal oxides and silicate impurities that helps in decreasing the %C.

Scanning electron microscope (SEM)

Insolubilized Azraq humic acid

From the SEM micrograph of INaAZHA (Fig. 4), the INaAZHA has an irregular shape, randomly distributed, partially melted, and plate like structure with very small pores.

In Figs. 5a and 6a for INaAZHA loaded with thorium and uranium respectively, thorium and uranium ions appear in bright color and randomly dispersed in different sites of INaAZHA.

Energy dispersive X-ray spectroscopy (EDS) of insolubilized Azraq humic acid with Th(IV) and U(VI)

The EDS for the insolubilized Azraq humic acid with the adsorbed thorium and uranium ions were done. The EDS results of thorium and uranium are shown in Figs. 5b and 6b respectively. The EDS give the type and weight percent of each element present in the selected point of sample at
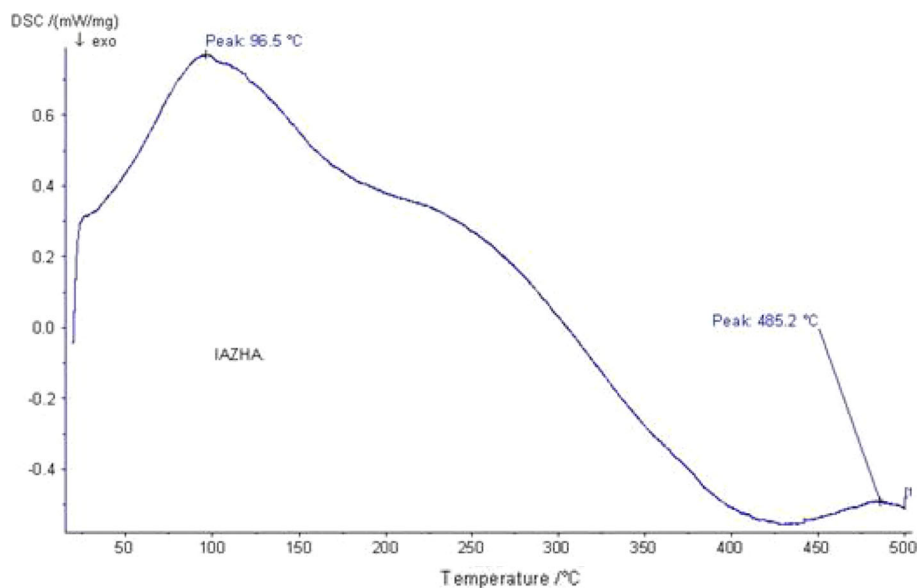

Fig. 2 TGA thermogram of INaAZHA

Fig. 3 DSC for INaAZHA

Table 2 Elemental analysis of INaAZHA, AZHA [14] and Ajloun IHA [10]

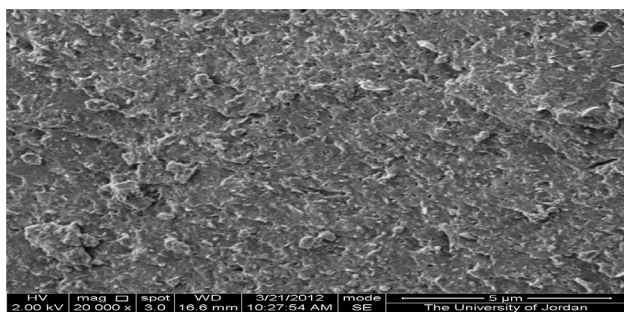| Site	% C	% N	% H
INaAZHA	48.08	2.02	3.86
Azraq HA	55.67	2.93	5.04
Ajloun IHA	23.04	1.03	2.73

Fig. 4 SEM micrographs for insolubilized Azraq humic acid with magnification ×20,000

SEM micrographs. From the EDS, the corresponding peaks for thorium and uranium appear in the INaAZHA sample in addition to other different elements. The percentage of each element after normalization is presented in Tables 3 and 4.

The amount of thorium in INaAZHA is more than the amount of uranium in INaAZHA this agrees with the sorption results. From Tables 3 and 4 we can observe that the %C in the case of thorium is lower than that in uranium, as stated above this due to the amount of adsorbed Th(IV) is higher than that of U(VI).

Kinetic of sorption

The plots of % uptake versus time for thorium(IV) and uranium(VI) by INaAZHA are shown in Fig. 7 for thorium and uranium respectively. We note from this Figure that Th(IV) and U(VI) needed 15 h to reach equilibrium at pH 3, and at 25.0, 35.0, and 45.0 °C. Al-Banna and Khalili [10] found that U(VI) and Th(IV) ions sorption by IHA from Ajloun need 6 h to reach equilibrium, at pH (1, 2, and 3), and 25.0 °C. Mohammed and Khalili [18] found that U(VI) and Th(IV) ion sorption by Azraq HA needed about 12 h to reach equilibrium, but Khalili et al. [4] found that U(VI) and Th(IV) ions sorption by Jordanian bentonite needed about 18 h to reach equilibrium at pH (1, 2, and 3), and 25.0 °C. Figure 8a, b showed the plots for pseudo-first order and pseudo-second order sorption kinetics.

From the difference between calculated and experimental q_e values (Table 5), it is seen that the sorption of Th(IV) and U(VI) onto INaAZHA is well described by the pseudo second order reaction kinetic. Moreover, all the correlation coefficients of pseudo second order reaction kinetic are higher than those of the pseudo first order reaction kinetic [28].

The activation energy of thorium is lower than that of uranium (Table 6), so the interaction of thorium is easier than uranium. The activation parameters of the sorption process help in predication of how the sorption of Th(IV) and U(VI) might vary with temperature changes. The activation energy, E_a, was 46.5 kJ mol^{-1} for Th(IV) and 54.9 kJmol^{-1} for U(VI), these values indicate that the sorption process is physisorption. The positive value of activation enthalpy confirms the endothermic process, meaning the reaction consume energy, the positive value of

Fig. 5 **a** SEM and **b** EDS for INaAZHA with thorium at ×10,000 magnifications
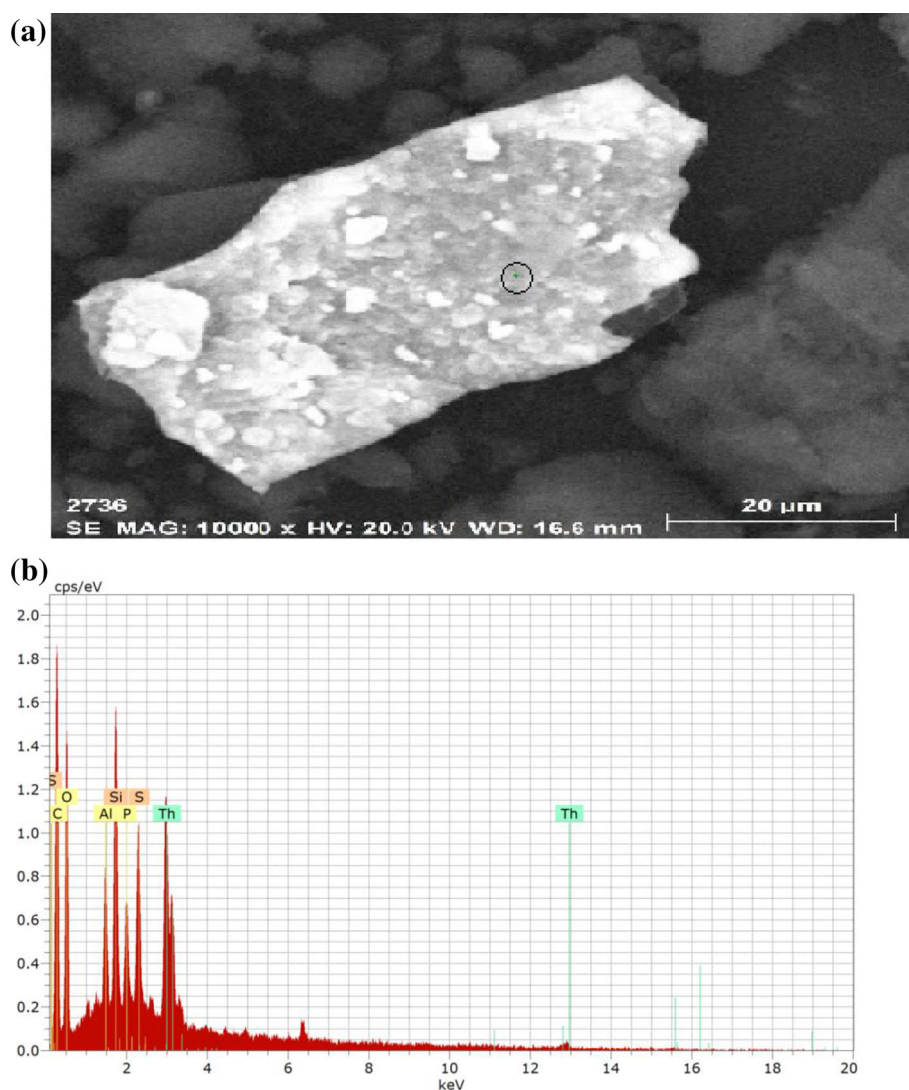
free energy of activation suggests that sorption reactions require energy to convert reactants into products, and the negative value of activation entropy indicates that the sorption leads to order through the formation of activated complex suggesting that Th(IV) and U(VI) sorption on INaAZHA is an associated mechanism [36].

Sorption studies of Th(IV) and U(VI) by INaAZHA

The sorption isotherms for the INaAZHA with Th(IV) and U(VI) ions Figs. 9a and 10a respectively as an example, have the L-isotherm. This means the ratio between the concentrations of the metal ions remaining in solution and adsorbed on the solid decreases when the solute (metal ions) concentration increases, suggesting the adsorbent has a high affinity for the adsorptive at low concentration [44]. But as the concentration increase, the affinity of the adsorptive will decrease because as more sites in the substrate (INaAZHA) are filled, it becomes increasingly

difficult for solute molecules to find a vacant site available [27, 45]. This result agrees with that obtained by Ajloun IHA towards these metal ions [10].

Langmuir isotherm will be used to estimate the sorption capacity, q_m and K_L, the Langmuir isotherms plots Fig. 9b for thorium and Fig. 10b for uranium, had excellent linearity. According to Langmuir model postulates this means the metal adsorbed on some sites whose binding energies are uniform and therefore formed a layer on the surface of the adsorbent, and there is no interaction between the adsorbed ions [46].

The values of q_m which related to sorption capacity indicated that increasing of temperatures and pH lead to increase in the sorption capacities of INaAZHA for metal ions. These results agree with that obtained from Table 7 for thorium uptake and Table 8 for uranium uptake with the same trend (Th(IV) > U(VI)).

The Freundlich isotherm plots are shown in Fig. 9c for thorium and Fig. 10c for uranium. The sorption of metal

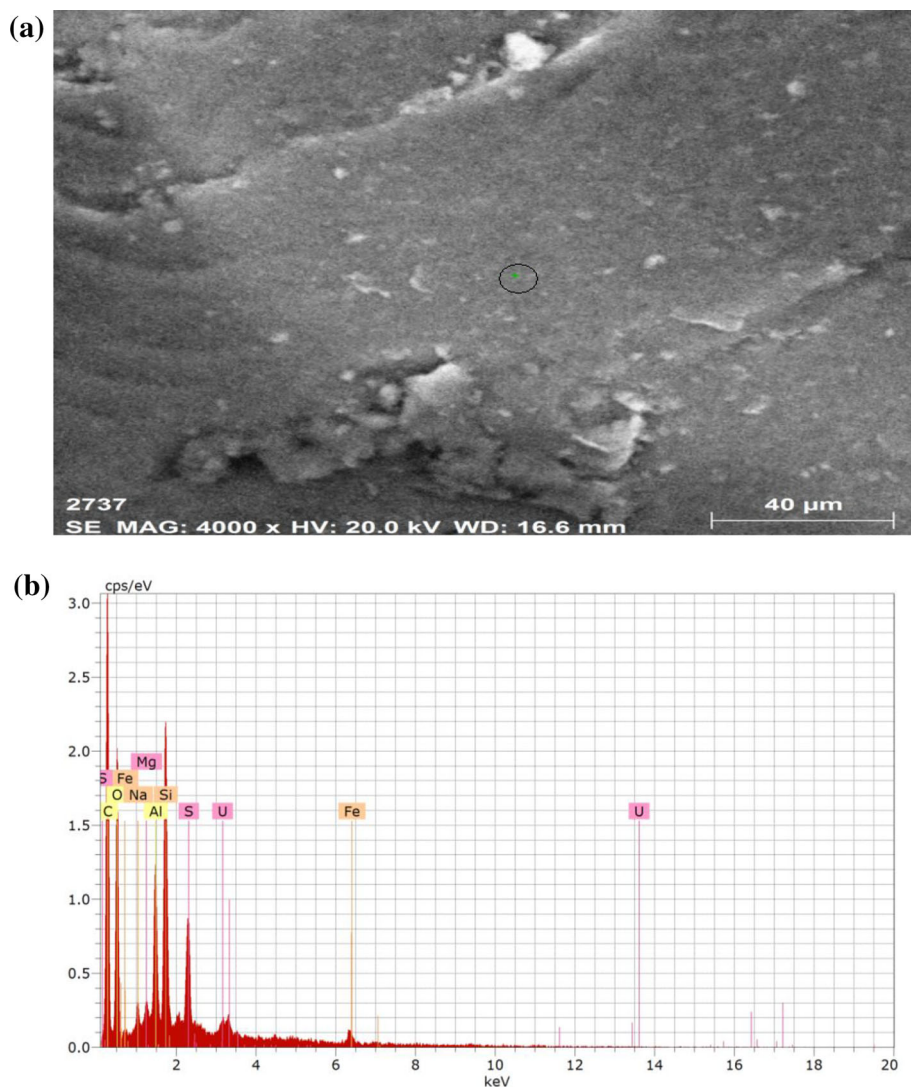**Fig. 6 a** SEM and **b** EDS for INaAZHA with uranium at ×4000 magnifications

(a)

(b)

Table 3 Normalized % mass of elements in INaAZHA loaded with thorium

Element	% Mass
C	30.79
O	53.30
Al	0.95
Si	1.78
P	0.88
S	1.48
Th	10.81

Fig. 7 Thorium(IV) and uranium(VI) percentage uptake by INaAZHA at 25, 35 and 45 °C at pH 3 and concentration of 30 ppm

Table 4 Normalized % mass of elements in INaAZHA loaded with uranium

Element	% Mass
C	33.54
O	52.83
Al	2.24
Si	3.36
S	1.53
Fe	1.67
U	3.77

ions on INaAZHA fitted Freundlich model, this model had excellent linearity. This means there is an indication that some other sorption sites were non–uniform and non-specific in nature. It was in conformity with the existence of different types of possible sorption sites on INaAZHA surface [47].

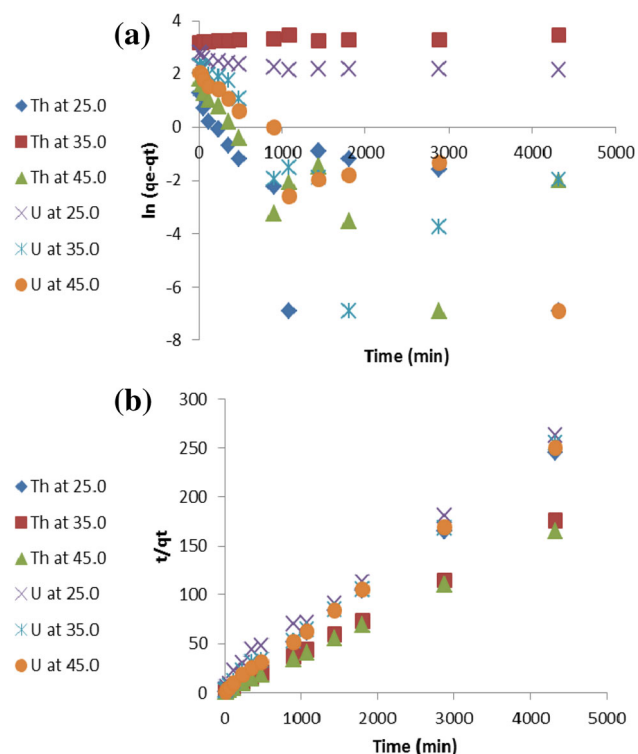**Fig. 8 a** Pseudo-first order sorption kinetics of thorium(IV) and uranium(VI) by INaAZHA at pH 1.0, 2.0 and 3.0 and concentration of 30 ppm. **b** Pseudo-second order sorption kinetics of thorium(IV) and uranium(VI) by INaAZHA at pH 1.0, 2.0 and 3.0 and concentration of 30 ppm

The values of n represent the degree of favorability of sorption. They were (Tables 7, 8) greater than one, indicating that the sorption was favorable [48]. The K_F values increase with increasing both temperature and pH for both metal ions (Tables 7, 8) and indicate that the sorption for Th(IV) is higher than U(VI).

The D–R isotherm model is more general than Langmuir isotherm as it rejects the homogenous surface or constant sorption potential. As illustrated in Table 7 for Th(IV) and

Table 8 for U(VI). The magnitude of E from D–R isotherm can give a good idea about the overall mechanism of the sorption. The values of E are less than 8.00 kJ mol^{-1}; this indicates that physical forces may affect the sorption [25]. It is interesting to note that the difference of q_m derived from the Langmuir and q'_m derived from D–R models is quite large. The difference may be attributed to the different definition of q_m in the two models. In Langmuir model, q_m represents the maximum sorption of metal ions at monolayer coverage, whereas in D–R model it represents the maximum sorption of metal ions at the total specific micropores volume of the sorbent. Thereby, the values of q_m derived from D–R model are lower than that derived from Langmuir model [29].

Comparing adsorptivity between Th(IV), and U(VI) at different conditions

According to the values of q_m in Tables 7 and 8, The removal capacity for metal ions by NaIHA was in the order of Th(IV) > U(VI). It indicated that NaIHA showed stronger preference for Th(IV) than U(VI).

We can explain these results as follows, where the adsorptivity of metal ions (q_m) on INaAZHA was found to be proportional to the ionic radius. In general, the most important factor that influences the relative selectivity of metal ions in solution is their ionic radii and the charge [49]. From Table 9, we can see that the ionic radius and charge for Th(IV) > U(VI), and the selectivity sequence observed is that Th(IV) adsorbed more than U(VI).

Hydration energy is another factor that has an important role in the sorption process of these metal ions, increasing the hydration energy values are due to the increase in the hydration shell, this makes it more difficult for metal ions to discharge the water of hydration. The formation of aqua complex $[M(H_2O)_m]^{n+}$ takes place

Table 5 Calculated and experimental q_e values for pseudo-first- and pseudo second- order sorption kinetics and k_2

Metal ion	Th(IV)			U(VI)		
	25.0 °C	35.0 °C	45.0 °C	25.0 °C	35.0 °C	45.0 °C
q_e calculated from pseudo 1st order kinetics (mg g^{-1})	1.652	4.884	3.880	13.550	7.541	7.709
q_e calculated from pseudo 2nd order kinetics (mg g^{-1})	17.483	24.691	26.316	16.807	17.986	17.699
q_e experimental	17.633	25.024	26.224	16.444	17.121	17.263
k_2 (g mg^{-1} min^{-1}) × 10^3	1.000	2.410	3.240	0.312	0.596	0.126

Table 6 Activation parameters for the sorption of Th(IV), and U(VI) onto INaAZHA

Metal ion	E_a (kJ mol^{-1})	$\Delta H^{\ddagger}$ (kJ mol^{-1})	$\Delta S^{\ddagger}$ (J mol^{-1} K^{-1})	$\Delta G^{\ddagger}$ (kJ mol^{-1})	A_2
Th(IV)	46.5	49.0	−42.5	61.7	1.50E+05
U(VI)	54.9	57.4	−25.1	64.9	1.30E+06

Fig. 9 Plots of **a** sorption isotherm of Th(IV), **b** linearized Langmuir, **c** linearized Freundlich, **d** D–R isotherm at pH 3.0 and 45.0 °C
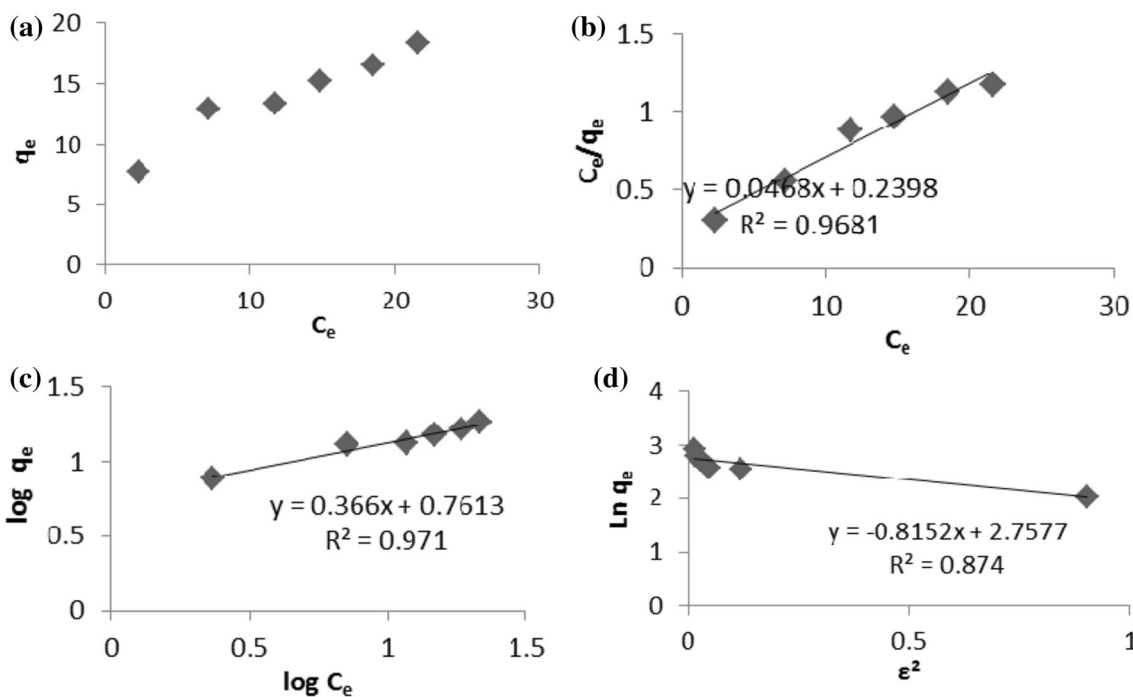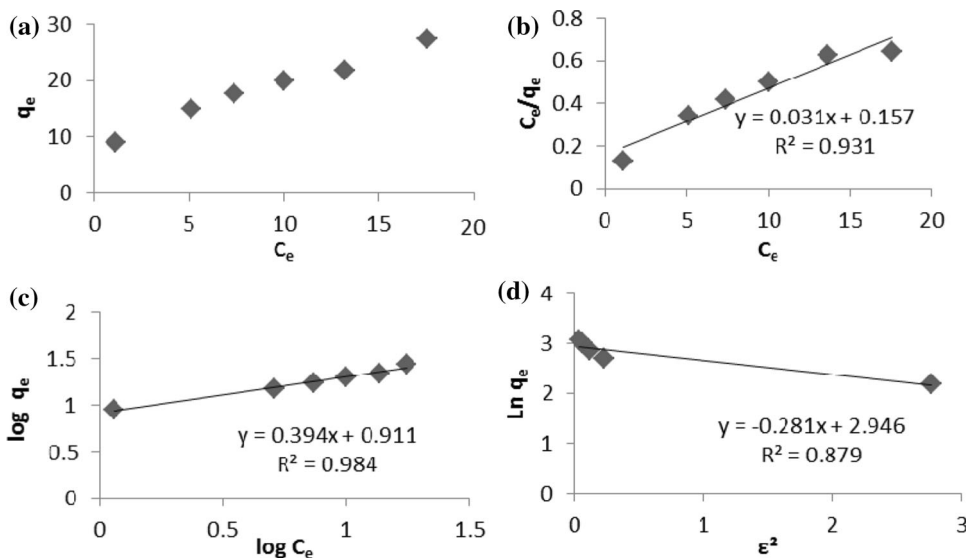

Fig. 10 Plots of **a** sorption isotherm of U(VI), **b** linearized Langmuir, **c** linearized Freundlich, **d** D–R isotherm at pH 3.0 and 45.0 °C

(where m is larger than six, perhaps eight or nine), the aqua complex, having m H_2O molecules surrounding the central metal ion, has a definite structure and the cloud of water molecules (hydration shell) has another geometry than the rest of the water [50]. A stronger hydration shell will surround small metal ion, which has smaller radius, than the metal ion with larger radius, so the adsorptivity of an ion of larger radius is higher than small radius ion. When it depends on the charge to size ratio; a large ratio results in an increase in hydration energy, which means

that the hydrated ion prefers the solution phase, where it may, satisfies its hydration requirements. Ions with lower hydration energy prefer the INaAZHA phase. Table 9 shows that uranium has higher hydration energy than thorium. This means that uranium exchange is more difficult at the INaAZHA surface.

According to Table 10 below we can note that the adsorptivity for INaAZHA is higher than that of Ajloun IHA and that of zeolite, but is lower than that for AZHA and Jordanian bentonite.

Table 7 Langmuir, Freundlich and Dubinin–Radushkevich (D–R) isotherms parameters for Azraq INaAZHA adsorbents towards Th(IV)

pH	T (°C)	Langmuir isotherm			Freundlich isotherm			D–R isotherm			
		r^2	q_m	K_L	r^2	n	K_F	r^2	β	E	q_m
1	25	0.924	11.236	0.044	0.982	1.773	0.939	0.954	6.990	0.267	5.818
	35	0.990	12.987	0.049	0.977	1.678	1.045	0.955	7.395	0.260	7.523
	45	0.978	20.833	0.043	0.988	1.558	1.371	0.916	5.512	0.301	10.528
2	25	0.978	14.124	0.106	0.984	2.458	2.771	0.849	2.668	0.433	9.508
	35	0.938	16.447	0.122	0.960	2.796	3.902	0.811	1.347	0.609	10.766
	45	0.994	21.978	0.144	0.990	2.278	4.475	0.911	1.383	0.601	15.424
3	25	0.944	25.316	0.146	0.986	2.576	5.851	0.887	0.711	0.703	15.518
	35	0.931	28.329	0.192	0.978	2.623	7.333	0.918	0.407	1.108	17.626
	45	0.931	31.949	0.199	0.984	2.539	8.153	0.879	0.281	1.334	19.020

Units for the parameters: K_L (L mg^{-1}), q_m (mg g^{-1}), K_F (L g^{-1}), β (mol^2 kJ^{-2}) and E (kJ mol^{-1})

Table 8 Langmuir, Freundlich and Dubinin–Radushkevich (D–R) isotherm parameters for Azraq INaAZHA adsorbents towards U(VI)

pH	T (°C)	Langmuir isotherm			Freundlich isotherm			D–R isotherm			
		r^2	q_m	K_L	r^2	n	K_F	r^2	β	E	q_m
1	25	0.967	8.197	0.067	0.931	1.931	0.962	0.981	8.305	0.245	5.601
	35	0.980	10.101	0.051	0.979	1.786	0.918	0.938	7.658	0.256	6.044
	45	0.993	10.753	0.055	0.984	1.799	1.028	0.947	6.740	0.272	6.593
2	25	0.967	17.544	0.088	0.930	1.946	2.388	0.970	4.315	0.340	11.905
	35	0.968	18.182	0.099	0.937	2.052	2.807	0.956	3.297	0.389	12.528
	45	0.985	19.608	0.100	0.941	2.004	2.917	0.967	2.973	0.410	13.289
3	25	0.997	18.051	0.199	0.974	2.732	4.875	0.941	1.416	0.594	14.055
	35	0.990	19.305	0.208	0.969	2.722	5.283	0.926	1.129	0.666	14.944
	45	0.968	21.739	0.192	0.971	2.732	5.768	0.874	0.815	0.783	15.753

Units for the parameters: K_L (L mg^{-1}), q_m (mg g^{-1}), K_F (L g^{-1}), β (mol^2 kJ^{-2}) and E (kJ mol^{-1})

Table 9 Chemical properties of Th(IV), and U(VI)

Metals	Th(IV)	U(VI)
Ionic radius (Å)	1.19	0.97
Hydration energy (kJ mol^{-1})	−3332	−3958

Thermodynamic results

Thermodynamics parameters such as free energy ($\Delta G°$), enthalpy change ($\Delta H°$) and entropy change ($\Delta S°$) were estimated using the following equations:

$$\Delta G° = -RT \ln K_d \quad (16)$$

$$\ln K_d = \Delta S°/R - \Delta H°/RT \quad (17)$$

where R is the gas constant (8.3145 J mol^{-1} K^{-1}), T is the temperature in Kelvin and K_d is the thermodynamic distribution coefficient, which can be defined as follows:

$$K_d = q_e/C_e \quad (18)$$

The ln K_d was calculated from the intercept of ln (q_e/C_e) versus q_e as shown in (Figs. 11, 12) for example [51].

In order to understand the sorption involved in the removal process. Thermodynamic functions for the system, including changes in Gibbs free energy, enthalpy of sorption and entropy of sorption, were calculated (Fig. 13), as shown in Table 11.

The Gibbs free energy indicates the degree of spontaneity of the sorption process, where more negative values reflect a more energetically favorable sorption process [52]. The negative values obtained in this study for INaAZHA confirm the feasibility of this adsorbent and spontaneity of the sorption. At pH 1 we note $\Delta G°$ values are small and positive, this indicates that the sorption is less favorable at low pH, and sorption of metal ions by INaAZHA needs small amount of energy to convert reactants into products [53].

The positive values of enthalpy change $\Delta H°$ show that the sorption of metal ions is endothermic. This means that as temperature increase, the sorption capacity was increased. This result agrees with results obtained in metal ions uptake, Table 7 for thorium and 8 for uranium, Langmuir parameter (q_m), Freundlich constant (K_F), and (q'_m values of D–R model. One possible explanation of the

Table 10 Comparing adsorptivity (q_m (mg g^{-1})) between Th(IV) and U(VI) ions at different pH and 45.0 °C on Ajloun IHA [10], AZHA [18], Jordanian zeolite [22] and Jordanian bentonite [4]

pH	Th(IV) Ajloun IHA	U(VI) Ajloun IHA	Th(IV) AZHA/ INaAZHA	U(VI) AZHA/ INaAZHA	Th(IV) Jordanian zeolite	U(VI) Jordanian zeolite	Th(IV) Jordanian bentonite	U(VI) Jordanian bentonite
1.00	20.41	9.80	38.98	15.71	13.50	5.30	35.97	17.83
			20.83	10.75				
2.00	21.74	18.87	75.18	67.36	17.50	11.00	101.01	39.22
			21.98	19.67				
3.00	35.71	25.64	191.20	149.24	18.10	16.50	135.14	53.48
			31.95	21.74				

endothermicity of heats of sorption is that the metal ions are well solvated. In order for the metal ions to be adsorbed, they have to lose part of their hydration sheath. This dehydration process of the ions requires energy. This energy of dehydration supersedes the exothermicity of the ions getting attach to the surface [25].

The positive values of $\Delta S°$ show the increased in randomness at the solid/solution interface during the sorption process. Positive entropy of sorption also reflects the affinity of adsorbent for metals used. The adsorbed water molecules, which are displaced by the adsorbate species, gain more translational energy than is lost by the adsorbate ions, thus allowing the prevalence of randomness in the system. Also, the dehydration of metal ions increases the randomness of the system [54]. Then, the positive entropy means that the sorption process increases the disorder of the system and it is entropy driven.

These results agree with that obtained from the sorption of Th(IV) and U(VI) ions by Ajloun IHA, but there is a small difference between the $\Delta G°$ values, where the values that obtained by the sorption of the same metal ions on Ajloun IHA are greater than that obtained in this study, this means the sorption process on INaAZHA is more spontaneous and most energetically favorable than that on Ajloun IHA [10].
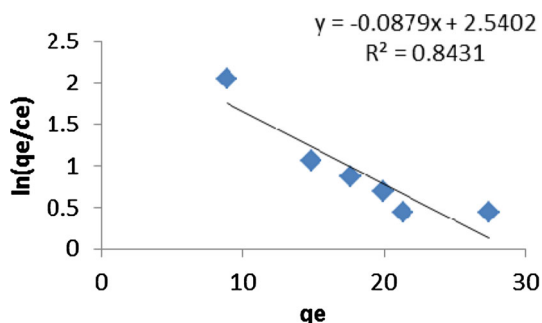

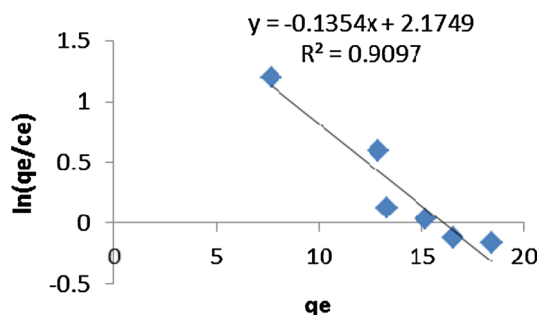**Fig. 12** Plot of ln (q_e/C_e) versus qe for U(VI) on INaAZHA at pH 3.0 and 45.0 °C
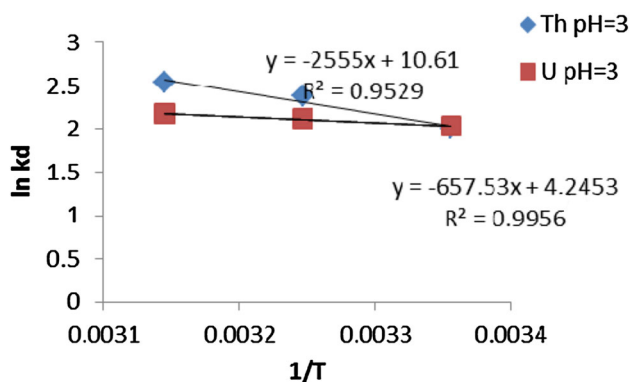

Fig. 13 Plots of ln K_d versus 1/T for thorium(IV) and uranium(VI) at pH 3.0

The effect of pH

It is clear as pH increases, sorption increases. This is noticed by the increased values of q_m with increasing pH, the sorption isotherm at pH 3.0 show the highest q_m value, as we can see in Fig. 14 which represents the values of q_m for Th(IV) and U(VI) metal ions respectively at different pH values. As the pH increases from 1.0 to 3.0 the degree of dissociation of carboxylate groups increases and the negative charge on INaAZHA increases, which will increase electrostatic interaction with metal ions, and the

Fig. 11 Plot of ln (q_e/C_e) versus q_e for Th(IV) on INaAZHA at pH 3.0 and 45.0 °C

Table 11 Thermodynamic Functions for sorption of Th(IV) and U(VI) by INaAZHA, these values were calculated at 25.0 °C

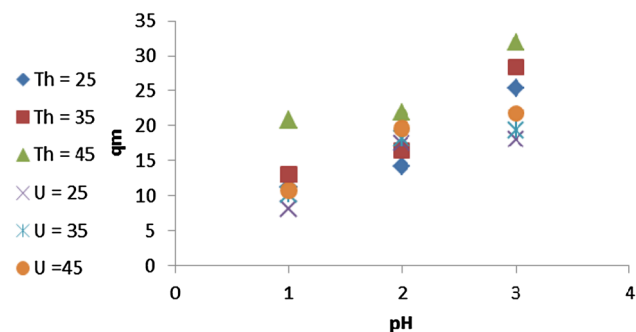| Metal ion	pH	$\Delta G°$ (kJ mol^{-1})	$\Delta H°$ (kJ mol^{-1})	$\Delta S°$ (J mol^{-1} K^{-1})
Th(IV)	1.00	1.34	20.54	64.26
	2.00	−2.34	27.35	100.01
	3.00	−4.97	21.25	88.25
U(VI)	1.00	1.25	6.54	17.74
	2.00	−1.40	13.73	50.75
	3.00	−5.05	5.47	35.303

Fig. 14 The pH dependence of q_m, pH 1.0, 2.0 and 3.0 at 25.0, 35.0, and 45.0 °C for Th(IV) and U(IV)

active sites of INaAZHA become more exposed to metal ion interaction.

Column experiments

Metal ion uptake by insolubilized Azraq humic acid

The investigation of metal ion uptake by the INaAZHA using column experiments for Th(IV) and U(VI) were determined at the optimum pH for each metal ion with initial concentration of 1000 ppm at room temperature (RT) and a flow rate of 0.50 mL min^{-1}. The results are expressed as percent metal uptake by the column and are presented in 12.

We can note that the uptake capacities of the metal ions fall in the order; Th(IV) < U(VI), these results agree with that of batch experiments (Table 12).

However, the values of percent uptake for the metal ions in column experiment are lower than those obtained in batch experiments at pH 3.00 and 25 °C, because in order to achieve complete saturation, long contact time is required. On the other hand, there is no mechanical shaking associated with column technique, which decrease the uptake of metal ions compared to batch experiments.

Desorption studies

Three different concentrations of nitric acid were used as eluting agents (1.0 M HNO$_3$, 0.5 M HNO$_3$, 0.1 M HNO$_3$), for the removal of metal ions, keeping the flow rate of elution 0.50 mL min^{-1}. The eluate was collected in five portions, 10.0 mL for each portion; the results are expressed as percent recovery and represented in Table 13.

Table 12 Metal ion uptake using column experiment at pH 3.00, and at RT

Metal ion	Initial concentration C_i (mg L^{-1})	Final concentration C_F (mg L^{-1})	Loaded concentration (mg L^{-1})	Uptake mg metal ion g^{-1} INaAZHA	% Uptake
Thorium(IV)	1000	572.4	427.6	10.7	42.8
Uranium(VI)	1000	595.8	404.2	10.1	40.4

Table 13 Desorption of Th(IV) and U(VI) ions from INaAZHA

Eluting agent	Th(IV)			U(VI)		
HNO$_3$	1.0 M	0.5 M	0.1 M	1.0 M	0.5 M	0.1 M
% Recovery first portion	34.1	27.8	25.7	37.5	29.7	27.4
% Recovery second portion	19.6	16.8	7.6	19.6	18.2	8.5
% Recovery third portion	12.0	8.1	5.6	13.3	9.1	5.6
% Recovery forth portion	9.2	7.5	4.8	8.3	7.8	4.7
% Recovery fifth portion	4.8	5.4	3.1	6.9	5.6	3.9
% Cumulative recovery	79.8	65.6	46.8	85.6	70.4	50.1

This experiment aims to determine the capability of INaAZHA regenerated for further uses. According to the values of the % cumulative recovery, in Table 13 the trend observed for eluting of metal ions from the INaAZHA is

$$1.0 \text{ M HNO}_3 > 0.5 \text{ M HNO}_3 > 0.1 \text{ M HNO}_3.$$

When concentration of HNO_3 is increased, desorption of Th(IV) and U(VI) increased because nitric acid acts as proton-exchanging agent. This agrees with the physical sorption nature rather than a chemical one [22].

Conclusions

The present work has focused on the extraction insolubilization, characterization, and sorption characteristics toward Th(IV) and U(VI). The structure of the insolubilized Azraq humic acid INaAZHA was confirmed by X-ray diffraction, Fourier transform infrared spectroscopy, thermogravimetric analysis, differential scanning calorimetry, elemental analysis, and scanning electron microscope. The sorption characteristics for Th(IV) and U(VI) ions from aqueous solutions were examined under various experimental conditions using both batch and column techniques. The effective desorption for the metal ions was studied, and the coefficient of recovery of sorption ability was also investigated.

As a result the following points were concluded:

- INaAZHA showed a relatively high uptake for Th(IV), and lower uptake for U(VI).
- The equilibrium for each metal ion on the surface of INaAZHA occurs at 15 h to achieve maximum uptake level.
- The metal ions sorption on INaAZHA is highly dependent of pH, that is, the adsorbed metal ions increased with increasing pH, and reached a maximum at pH 3 for both metal ions.
- The thermodynamic parameters show that the sorption process is favorable, and the sorption of metal ions is an endothermic process.
- The activation parameters show that the mechanism of sorption is associated mechanism, and indicate that sorption process is physisorption one.
- The obtained sorption data showed fitting for Langmuir, Freundlich, Dubinin–Radushkevich sorption isotherm models with good correlation coefficients.
- A column packed with the INaAZHA has good metal uptake properties toward metal ions, and followed the order: Th(IV) > U(VI), at pH 3, RT. and flow rate of 0.50 mL min^{-1}.
- The efficiency of recovery of the metal ions after sorption can be carried out by treatment of the loaded

INaAZHA with 1.0 M HNO_3 with good percent recovery.

References

1. Majdan M, Pikus S, Gajowiak A, Gładysz-Płaska A, Krzyżanowska H, Żuk J, Bujacka M (2010) Characterization of uranium(VI) sorption by organobentonite. Appl Surf Sci 256(17):5416–5421. doi:10.1016/j.apsusc.2009.12.123
2. Anirudhan TS, Rijith S, Tharun AR (2010) Adsorptive removal of thorium(IV) from aqueous solutions using poly(methacrylic acid)-grafted chitosan/bentonite composite matrix: process design and equilibrium studies. Colloids Surf A 368(1–3):13–22. doi:10.1016/j.colsurfa.2010.07.005
3. Seyhan S, Merdivan M, Demirel N (2008) Use of o-phenylene dioxydiacetic acid impregnated in Amberlite XAD resin for separation and preconcentration of uranium(VI) and thorium(IV). J Hazard Mater 152(1):79–84. doi:10.1016/j.jhazmat.2007.06.065
4. Khalili FI, NaH Salameh, Shaybe MM (2013) Sorption of uranium(VI) and thorium(IV) by Jordanian bentonite. J Chem 2013:13. doi:10.1155/2013/586136
5. Saqan SA, Kullab MK, Ismail AM (2001) Radionuclides in hot mineral spring waters in Jordan. J Environ Radioact 52(1):99–107. doi:10.1016/S0265-931X(00)00096-5
6. Anirudhan TS, Radhakrishnan PG (2009) Improved performance of a biomaterial-based cation exchanger for the adsorption of uranium(VI) from water and nuclear industry wastewater. J Environ Radioact 100(3):250–257. doi:10.1016/j.jenvrad.2008.12.006
7. Baker H, Khalili F (2004) Analysis of the removal of lead(II) from aqueous solutions by adsorption onto insolubilized humic acid: temperature and pH dependence. Anal Chim Acta 516(1–2):179–186. doi:10.1016/j.aca.2004.03.068
8. Baybaş D, Ulusoy U (2011) The use of polyacrylamide-aluminosilicate composites for thorium adsorption. Appl Clay Sci 51(1–2):138–146. doi:10.1016/j.clay.2010.11.020
9. Yusan S, Akyil S (2008) Sorption of uranium(VI) from aqueous solutions by akaganeite. J Hazard Mater 160(2–3):388–395. doi:10.1016/j.jhazmat.2008.03.009
10. Khalili F, Al-Banna G (2015) Adsorption of uranium(VI) and thorium(IV) by insolubilized humic acid from Ajloun soil–Jordan. J Environ Radioact 146:16–26. doi:10.1016/j.jenvrad.2015.03.035
11. Choudhry GG (1984) Humic substances. Structural, photophysical, photochemical and free radical aspects and interactions with environmental chemicals. Gordon & Breach Science Publishers Inc., New York
12. Ngah WSW, Fatinathan S, Yosop NA (2011) Isotherm and kinetic studies on the adsorption of humic acid onto chitosan-H$_2$SO$_4$ beads. Desalination 272(1–3):293–300. doi:10.1016/j.desal.2011.01.024
13. Santosa SJ, Siswanta D, Sudiono S, Sehol M (2007) Synthesis and utilization of chitin–humic acid hybrid as sorbent for Cr(III). Surf Sci 601(22):5148–5154. doi:10.1016/j.susc.2007.04.161
14. Khalili F (1987) Humic and fulvic acids from several locations in Jordan. Dirasat 14(12):151–162
15. Khalili F, Ajjourni H (1987) X-ray diffraction studies on Jordanian humic and fulvic acids. Dirasat 14:163–167
16. Khalili F (1988) The nature of the Azraq Oasis humic acid. J Iraqi Chem Soc 13:71–85

17. El-Eswed B, Khalili F (2006) Adsorption of Cu (II) and Ni (II) on solid humic acid from the Azraq area, Jordan. J Colloid Interface Sci 299(2):497–503

18. Mohammad A, Khalili F (2012) Adsorption of thorium (IV) and uranium (VI) onto Azraq humic acid, Jordan

19. Celebi O, Kilikli A, Erten H (2009) Sorption of radioactive cesium and barium ions onto solid humic acid. J Hazard Mater 168(2):695–703

20. D-Q Pan, Q-H Fan, Li P, Liu S-P, Wu W-S (2011) Sorption of Th(IV) on Na-bentonite: effects of pH, ionic strength, humic substances and temperature. Chem Eng J 172(2):898–905

21. Gezici O, Kara H, Ayar A, Topkafa M (2007) Sorption behavior of Cu (II) ions on insolubilized humic acid under acidic conditions: an application of Scatchard plot analysis in evaluating the pH dependence of specific and nonspecific bindings. Sep Purif Technol 55(1):132–139

22. Al-Shaybe M, Khalili F (2009) Adsorption of thorium (IV) and uranium (VI) by tulul al-shabba zeolitic tuff, Jordan. Jordan J Earth Environ Sci 2:108–119

23. Talip Z, Eral M, Hiçsönmez Ü (2009) Adsorption of thorium from aqueous solutions by perlite. J Environ Radioact 100(2):139–143

24. Ünlü N, Ersoz M (2006) Adsorption characteristics of heavy metal ions onto a low cost biopolymeric sorbent from aqueous solutions. J Hazard Mater 136(2):272–280

25. Donat R, Akdogan A, Erdem E, Cetisli H (2005) Thermodynamics of Pb 2+ and Ni 2+ adsorption onto natural bentonite from aqueous solutions. J Colloid Interface Sci 286(1):43–52

26. Abdullah M, Chiang L, Nadeem M (2009) Comparative evaluation of adsorption kinetics and isotherms of a natural product removal by Amberlite polymeric adsorbents. Chem Eng J 146(3):370–376

27. Stevenson FJ (1994) Humus chemistry: genesis, composition, reactions. Wiley, New York

28. Veli S, Alyüz B (2007) Adsorption of copper and zinc from aqueous solutions by using natural clay. J Hazard Mater 149(1):226–233

29. Xu D, Tan X, Chen C, Wang X (2008) Adsorption of Pb(II) from aqueous solution to MX-80 bentonite: effect of pH, ionic strength, foreign ions and temperature. Appl Clay Sci 41(1):37–46

30. Kütahyalı C, Eral M (2010) Sorption studies of uranium and thorium on activated carbon prepared from olive stones: kinetic and thermodynamic aspects. J Nucl Mater 396(2):251–256

31. Bhattacharyya KG, Gupta SS (2008) Adsorption of a few heavy metals on natural and modified kaolinite and montmorillonite: a review. Adv Colloid Interface Sci 140(2):114–131

32. Ho YS, McKay G (1998) Sorption of dye from aqueous solution by peat. Chem Eng J 70(2):115–124. doi:10.1016/S0923-0467(98)00076-1

33. Petrou AL, Economou-Eliopoulos M (2009) The activation energy values estimated by the Arrhenius equation as a controlling factor of platinum-group mineral formation. Geochim Cosmochim Acta 73(6):1625–1636

34. Doğan M, Abak H, Alkan M (2009) Adsorption of methylene blue onto hazelnut shell: kinetics, mechanism and activation parameters. J Hazard Mater 164(1):172–181

35. Al-Ghouti M, Khraisheh M, Ahmad M, Allen S (2005) Thermodynamic behaviour and the effect of temperature on the removal of dyes from aqueous solution using modified diatomite: a kinetic study. J Colloid Interface Sci 287(1):6–13

36. Petrou AL (2012) The free energy of activation as the critical factor in geochemical processes. Chem Geol 308:50–59

37. Savvin S (1961) Analytical use of arsenazo III: determination of thorium, zirconium, uranium and rare earth elements. Talanta 8(9):673–685

38. Khalili F, Al-Taweel S, Yousef Y, Al-Tarawneh S (2008) Synthesiss characterization and solvent extraction properties of new thiophene based trifluoromethyl-substituted B-diketones for thorium (IV) and uranium (VI) Ions. J Saudi Chem Soc 12(2):165–176

39. Khalili F (1993) Lead (II) complexation by Azraq humic acid. Muta'h Lil-Buhooth wa Al-Dirasat 8(1):121–135

40. El-Eswed BI (2005) Adsorption of heavy metals by humic acid from Azraq area. University of Jordan, Amman

41. Chen H, Berndtsson R, Ma M, Zhu K (2009) Characterization of insolubilized humic acid and its sorption behaviors. Environ Geol 57(8):1847–1853

42. Kolokassidou C, Pashalidis I, Costa C, Efstathiou A, Buckau G (2007) Thermal stability of solid and aqueous solutions of humic acid. Thermochim Acta 454(2):78–83

43. Chilom G, Rice JA (2005) Glass transition and crystallite melting in natural organic matter. Org Geochem 36(10):1339–1346

44. Limousin G, Gaudet J-P, Charlet L, Szenknect S, Barthes V, Krimissa M (2007) Sorption isotherms: a review on physical bases, modeling and measurement. Appl Geochem 22(2):249–275

45. Giles CH, MacEwan TH, Nakhwa SN, Smith D (1960) 786. Studies in adsorption. Part XI. A system of classification of solution adsorption isotherms, and its use in diagnosis of adsorption mechanisms and in measurement of specific surface areas of solids. J Chem Soc (Resumed). doi:10.1039/JR9600003973

46. Adebowale K, Unuabonah I, Olu-Owolabi B (2005) Adsorption of some heavy metal ions on sulfate-and phosphate-modified kaolin. Appl Clay Sci 29(2):145–148

47. Jiang M-Q, Jin X-y, Lu X-Q, Chen Z-l (2010) Adsorption of Pb(II), Cd (II), Ni (II) and Cu (II) onto natural kaolinite clay. Desalination 252(1):33–39

48. Unuabonah E, Adebowale K, Olu-Owolabi B, Yang L, Kong L (2008) Adsorption of Pb(II) and Cd (II) from aqueous solutions onto sodium tetraborate-modified Kaolinite clay: equilibrium and thermodynamic studies. Hydrometallurgy 93(1):1–9

49. Puls RW, Bohn HL (1988) Sorption of cadmium, nickel, and zinc by kaolinite and montmorillonite suspensions. Soil Sci Soc Am J 52(5):1289–1292

50. Sinha SP (2013) Complexes of the rare earths. Elsevier, Amsterdam

51. Boparai HK, Joseph M, O'Carroll DM (2011) Kinetics and thermodynamics of cadmium ion removal by adsorption onto nano zerovalent iron particles. J Hazard Mater 186(1):458–465

52. Dakiky M, Khamis M, Manassra A, Mer'eb M (2002) Selective adsorption of chromium (VI) in industrial wastewater using low-cost abundantly available adsorbents. Adv Environ Res 6(4):533–540

53. Scheckel KG, Sparks DL (2001) Temperature effects on nickel sorption kinetics at the mineral–water interface. Soil Sci Soc Am J 65(3):719–728

54. Güzel F, Yakut H, Topal G (2008) Determination of kinetic and equilibrium parameters of the batch adsorption of Mn(II), Co (II), Ni (II) and Cu (II) from aqueous solution by black carrot (Daucus carota L.) residues. J Hazard Mater 153(3):1275–1287